ANALYTIC MODEL FOR PERFORATED SQUEEZED-FILM DAMPERS

T. Veijola

DTIP of MEMS & MOEMS Stresa, Lago Maggiore, Italy, 26-28 April 2006

ANALYTIC MODEL FOR PERFORATED SQUEEZED-FILM DAMPERS

Timo Veijola

Helsinki University of Technology, P.O. Box 3000, FIN-02015 HUT, Finland,
email: timo.veijola@hut.fi, tel. +358 9 451 2293, fax. +358 9 451 4818.

ABSTRACT

The concept of a perforation cell to derive simple analytic models for perforated squeezed-film dampers is applied. The perforation cell models the cylindrical volume around a single perforation. An extended Reynolds equation is then used to model the damping due both to the gas flow in the air gap and in the perforations. The method is applied in a rectangular damper with $4 \ldots 64$ square holes to derive the damping coefficient analytically. 3D FEM simulations are used to verify the model. The damping predicted by the model is in good agreement with that obtained with 3D FEM simulations.

Sinusoidal small-amplitude velocities are assumed, and micromechanical dimensions are considered with rare gas effects in the slip flow regime ($K_\mathrm{n} < 0.1$).

1. INTRODUCTION

Perforations are used in several MEMS devices including microphones, capacitive switches resonators, and accelerometers, since they reduce damping in a squeezed-film structure considerably.

Modelling of perforated structures is problematic because of the complexity of their geometries: a perforated surface might consist of thousands of tiny holes. Direct simulation of such structures with FEM tools often fails since the simulation problem becomes too large and slow. The small dimensions of the micromechanical structures (about 1μm) is another challenge for modelling; the rare gas effects become important even at ambient pressures. The models that are valid for the continuum flow regime are no longer sufficient.

Perforated dampers are usually made of a perforation grid. When this grid is uniform, and the holes are large enough, a repetitive pressure pattern forms around each hole. This will be utilized in modelling perforated dampers: the flow problem is isolated in a cylindrical region around a single perforation, a *perforation cell*. This simplifies the analysis, and also compact, parameterized macro models for these perforation cells can be derived.

Analytic models for such perforation cells have been presented in the literature [1], [2], [3], [4], and [5]. Unfortunately, none of these contains proper models for the fringe flows, and the reported models are not properly verified. In [6] a model for a cylindrical perforation cell is derived based on FEM simulations.

A model is often needed for the case when a considerable amount of gas flows from the damper borders. In this case, the pressure profile is no longer repetitive, and the perforation cell alone is not sufficient in modelling the damping. The problem can be formulated as an extended Reynolds equation that has an additional "leakage" term due to perforation [2]. The great benefit here is that the problem is reduced now to 2D. There are two alternate ways to solve this equation with FEM tools: a homogenization approach, where the leakage due to perforation is homogenized uniformly on the damper surface [2], [7], [8], and a "Perforation Profile Reynolds" (PPR) method [9], where the leakage is described as a spatially variable perforation profile. In this paper, the homogenization approach has been used to derive an analytic compact model for perforated dampers. The perforation cell model derived in [6] is applied to calculate the "leakage" term needed in the extended Reynolds equation.

2. PERFORATION CELL

Figure 1 shows the topology of the perforation cell. It is assumed that the radius of this cell is r_x (about half of the perforation pitch) and the radius of the hole is r_0.

2.1. Perforation Cell Model

Figure 2 shows the lumped flow resistances, that are used to model the flow resistance (mechanical resistance) of the cell.

It is equivalent to the force F acting on the bottom surface divided by the velocity of the bottom surface,

 ISBN: 2-916187-03-0

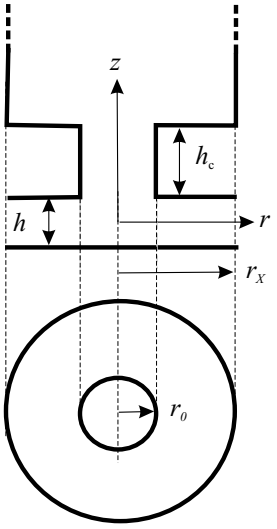

Figure 1: Topology and dimensions of the axisymmetric perforation cell.

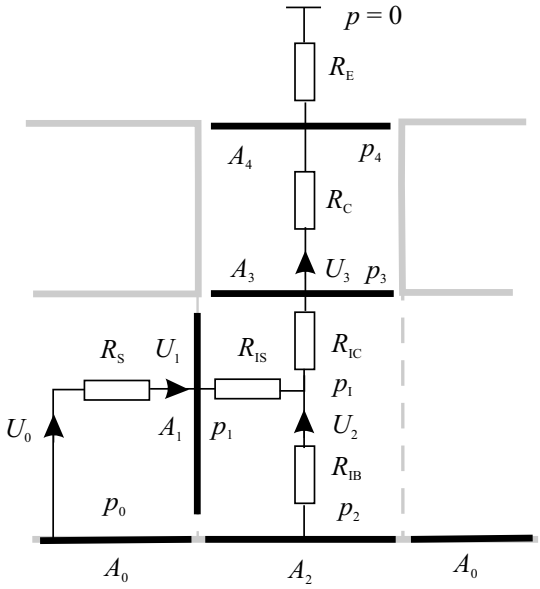

Figure 2: Lumped flow resistances used in modelling the flow in different regions of a perforation cell.

$R_\mathrm{P} = F/v_\mathrm{z}$, i. e.,

$$R_\mathrm{P} = R_\mathrm{S} + R_\mathrm{IS} + R_\mathrm{IB} + \frac{r_\mathrm{x}^4}{r_0^4}\left(R_\mathrm{IC} + R_\mathrm{C} + R_\mathrm{E}\right). \quad (1)$$

The resistances R_S and R_C are derived analytically, but the remaining resistances, that model the fringe flows, are derived from FEM simulations in [6]. The equations for the flow resistances in Eq. (1) are given in Appendix.

The validity of the perforation cell model in [6] is limited to cases where $K_\mathrm{n} < 0.1$, $r_0/h < 4$, and $r_0/r_\mathrm{x} < 0.95$. If the intermediate flow resistances in Eq. (1) are ignored, if reduces to the model presented in [3], [4].

2.2. Rare Gas Effects

The Knudsen number $\mathtt{Kn} = \lambda/a$ is a measure of gas rarefaction. It is the ratio between the mean free path λ and the nominal displacement a. Since λ is inversely proportional to pressure, Kn increases when the pressure drops below the ambient pressure. In this paper, two different Knudsen numbers are used: one for the channel flow in the air gap K_ch, and one for the capillary flow in the perforation K_tb. Here, we include also the effect of the surface condition into the Knudsen number.

For the channel flow

$$K_\mathrm{ch} = \frac{\sigma_\mathrm{P}\lambda}{h}, \quad (2)$$

where h is the air gap height, and for the capillary flow

$$K_\mathrm{tb} = \frac{\sigma_\mathrm{P}\lambda}{r_0}, \quad (3)$$

where r_0 is the radius of the capillary. For the diffuse-specular scattering model [10], σ_P is specified as

$$\sigma_\mathrm{P} = \frac{2-\alpha}{\alpha}[1.016 - 0.1211(1-\alpha)], \quad (4)$$

where α is the momentum accommodation coefficient. For diffuse scattering, $\alpha = 1$, and σ_P reduces to 1.016.

The damping in the structure will change through the relative flow rate coefficients, that depend on the Knudsen numbers. In the slip flow regime these are

$$Q_\mathrm{ch} = 1 + 6K_\mathrm{ch} \quad (5)$$

for the flow in the air gap and

$$Q_\mathrm{tb} = 1 + 4K_\mathrm{tb} \quad (6)$$

for the flow in perforations with circular cross-sections.

3. MODEL FOR PERFORATED DAMPER

3.1. Extended Reynolds Equation

The homogenization principle is used to combine the vertical flow in the air gap escaping from the damper borders with the flow through the perforations. The model derived from the extended Reynolds equation presented in [2] is used, and the edge effect model is adopted from [11]. This extension contains an additional term $p/(NR_\mathrm{P})$ in the Reynolds equation that

 ISBN: 2-916187-03-0

models the flow through N perforations. R_P is the flow resistance of a single perforation, modelled here with the perforation cell model given in Eq. (1). The extended Reynolds equation without compressibility effects can be written as

$$\frac{h^3 Q_\mathrm{ch}}{12\eta}\left(\frac{\partial^2 p}{\partial x^2}+\frac{\partial^2 p}{\partial y^2}\right)-\frac{p}{NR_\mathrm{P}}=v_\mathrm{z}, \qquad (7)$$

where p is the pressure variation (function of x and y) and η is the viscosity coefficient.

Equation 7 can be generally solved with FEM methods, but for simple geometries it can be solved also analytically.

3.2. Rectangular Damper

The perforation cell model is applied here in building a simple model for a perforated damper with rectangular surfaces ($a \times b$) in perpendicular motion. Uniform perforation is assumed.

It is necessary to correct for the edge effects if the ratio $a/h < 50$ [11]. The effective surface dimensions modelling the edge effects in the slip flow regime are

$$a_\mathrm{eff} = a + 1.3(1+3.3K_\mathrm{ch})h, \qquad (8)$$
$$b_\mathrm{eff} = b + 1.3(1+3.3K_\mathrm{ch})h. \qquad (9)$$

The pressure function satisfying Eq. (7) is

$$p=\sum_{m,n} c_{m,n}\cos(m\pi x/a_\mathrm{eff})\cos(n\pi y/b_\mathrm{eff}) \qquad (10)$$

where n and n and positive indices. The coefficients $c_{m,n}$ are determined from the boundary conditions. The velocity of the surface is also expressed with a Fourier series:

$$v_\mathrm{z}=v_\mathrm{r}\sum_{m,n} h_{m,n}\cos(m\pi x/a_\mathrm{eff})\cos(n\pi y/b_\mathrm{eff}) \qquad (11)$$

where $h_{m,n} = 16/(mn\pi^2)$ for perpendicular motion. After inserting Eqs. (10) and (11) into Eq. (7), coefficients $c_{m,n}$ are solved:

$$c_{m,n}=\frac{-h_{m,n}v_\mathrm{r}}{\frac{h^3 Q_\mathrm{ch}\pi^2}{12\eta}\left(\frac{m^2}{a_\mathrm{eff}^2}+\frac{n^2}{b_\mathrm{eff}^2}\right)+\frac{1}{NR_\mathrm{P}}} \qquad (12)$$

Integration over the surface gives the total pressure

$$p_{tot}=\int_{-a_\mathrm{eff}/2}^{a_\mathrm{eff}/2}\int_{-b_\mathrm{eff}/2}^{b_\mathrm{eff}/2} p\,\mathrm{d}x\mathrm{d}y \qquad (13)$$

The mechanical resistance of the damper is $R_\mathrm{D} = -p_{tot}/v_\mathrm{r}$

$$R_\mathrm{D}=\sum_{m,n}\frac{1}{G_{m,n}+\frac{1}{R_{m,n}}},\quad \begin{cases} m=1,3,5,\ldots, \\ n=1,3,5,\ldots, \end{cases} \qquad (14)$$

where

$$G_{m,n}=\left(\frac{m^2}{a_\mathrm{eff}^2}+\frac{n^2}{b_\mathrm{eff}^2}\right)\frac{m^2n^2\pi^6h^3Q_\mathrm{ch}}{768\eta a_\mathrm{eff}b_\mathrm{eff}}, \qquad (15)$$

and

$$R_{m,n}=\frac{64NR_\mathrm{P}}{m^2n^2\pi^4}. \qquad (16)$$

The indices m and n in Eq. (14) run to infinity, but for an accuracy better than 1 %, a maximum value of 15 for m and n is sufficient (for a square surface).

4. VERIFICATION

Several perforated dampers in perpendicular motion are characterized with full 3D Navier-Stokes simulations. The surface is a square, and the perforation consists of identical square holes. The number of holes N varies from 4 to 64. The simulated flow resistance is compared with the simple model given in Eq. (14).

The topology of one of the four different simulated structures is shown in Fig. 3 ($N = 16$). Square hole dimensions and cell peripheries are accounted for by specifying effective radii r_x and r_0. Radius $r_\mathrm{x} = 0.5 s_\mathrm{x}\sqrt{4/\pi}$ is selected such that the areas of the circular and square shapes match. Radius r_0 results from equating the hydraulic resistances (acoustic resistances) of square and circular capillaries:

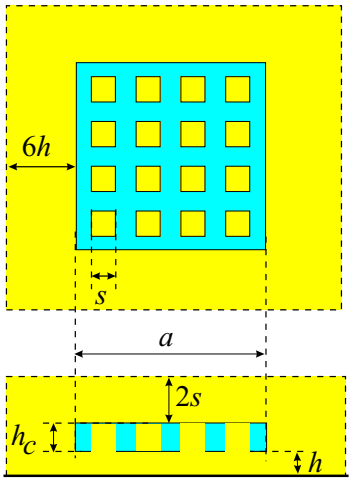

Figure 3: Structure of simulated dampers. Topology with $N = 16$ holes is shown. The figure also illustrates the simulation space around the structure in the 3D Navier-Stokes simulations.

$$r_0=\left(\frac{128Q_\mathrm{sq}}{28.454\pi Q_\mathrm{tb}}\right)^{\frac{1}{4}}\frac{s}{2}\approx 1.096\cdot\frac{s}{2}, \qquad (17)$$

where s is the width of each hole and Q_sq is the relative flow rate of square perforation. The approxima-

 ISBN: 2-916187-03-0

tion assumes that the difference between Q_{tb} and Q_{sq} is small.

4.1. 3D FEM Simulations

3D FEM simulations with Navier-Stokes solver are performed for the structures and the free air around it. The multiphysical FEM software Elmer [12] was used. The simulations were performed here relatively reliably, thanks to the small number of holes and the symmetry in the structure (actually, one quarter of the structure was simulated). The simulated gas volume was extended around the damper: free space around and above the damper are $6h$ and $2s$, respectively. A mesh of 500 000 elements is used, and slip boundary conditions are used for the surfaces. The constant velocity v_{z} is set to 1 m/s.

The comparison was made well below the cut-off frequency, that is, the compressibility and inertia of the gas were ignored. The dimensions and parameters are summarized in Table 1.

Table 1: Dimensions and parameters for the simulated perforated dampers. In all cases, the perforation pitch is $s_{\mathrm{x}} = 5\,\mu$m. Altogether, 288 different topologies were generated and simulated.

	Description	Value	Unit
N	number of holes	4, 16, 36, 64	
a	surface length	10, 20, 30, 40	10^{-6} m
s	hole width	0.5, 1, ..., 4.5	10^{-6} m
h_{c}	thickness	0.5, 1, 2, 5	10^{-6} m
h	air gap height	1, 2	10^{-6} m
η	viscosity coeff.	20	10^{-6} Ns/m^2
λ	mean free path	69	10^{-9} m
σ_{P}	slip coefficient	1	

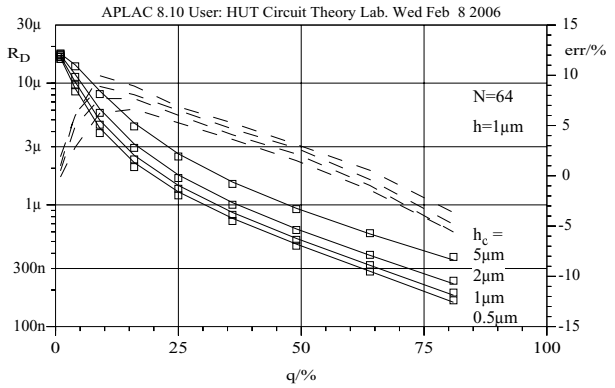

a)

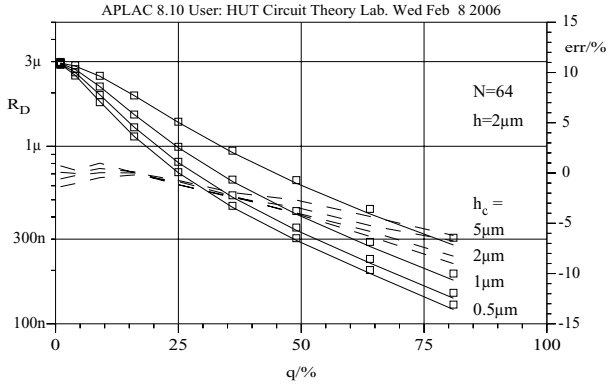

b)

Figure 4: Simulated (□) and approximated (——) flow resistance of the perforated damper as a function of the perforation ratio q. The number of perforations is 64 and the air gap height is a) $h = 1\,\mu$m and b) $h = 2\,\mu$m. The relative error is also shown (– – –) on the right-hand scale.

4.2. Results

Figures 4 and 5 compare the FEM simulations and the model response as a function of the perforation ratio $q = s^2/s_{\mathrm{x}}^2 \cdot 100\%$ when $N = 64$ and $N = 36$, respectively. The accuracy of the model is good, the maximum relative error is less than 12 %. The other simulations show similar behaviour, but the error increases when the number of holes decreases. The maximum relative errors are 10 %, 12 %, 20 %, and 35 % for N of 64, 36, 16, and 4, respectively. The use of the effective surface dimensions, Eqs (8) and (9), to model the edge effects results in a small error even for ratios of a/h as low as 20.

The maximum relative error was about 35 % for the damper with four holes. Such an error was expected, because, in this case, the validity of the perforation cell approach is questionable. The error is mostly due to the fringe forces acting on the sidewalls and on the top surface of the damper that are excluded from the model presented. The error in the model was the greatest for large perforation ratios, where the damping is at its minimum, and the relative contribution of the fringe effects dominates. Also, approximating the rectangular hole with a circular equivalent in Eq. (17) may be a source of an error that increases with the perforation ratio.

 ISBN: 2-916187-03-0

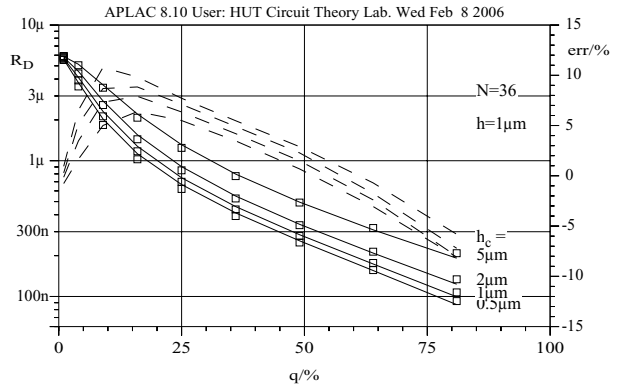

a)

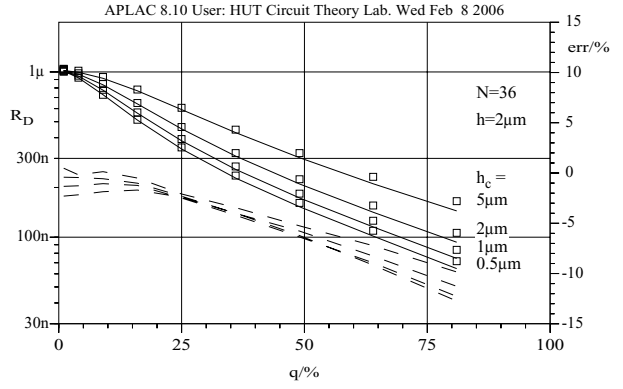

b)

Figure 5: Simulated (□) and approximated (——) flow resistance of the perforated damper as a function of the perforation ratio q. The number of perforations is 36 and the air gap height is a) $h = 1\,\mu$m and b) $h = 2\,\mu$m. The relative error is also shown (– – –) on the right-hand scale.

5. CONCLUSIONS

A relatively simple model is derived here for uniformly perforated, rectangular dampers. This model was verified against 3D FEM simulations in the slip flow regime. The model shows good accuracy (better than 10 %) for a damper with 64 holes, but the relative error increases when the number of holes is reduced. The accuracy is good due to the fringe resistances in the model, and due to the included edge effects. This simple model could be improved by taking into account the effect of the flow past the holes in the air gap. Also, the fringe flows around the damper should be included in the damper model, especially if a/h is not large. It is straightforward to implement this model to any software tool, since the model consists of simple equations.

REFERENCES

[1] Z. Skvor, "On the Acoustic Resistance Due to Viscous Losses in Air Gap of Electrostatic Transducers," *Acoustica*, vol. 19, pp. 295–299, 1967.

[2] T. Veijola and T. Mattila, "Compact Squeezed-Film Damping Model for Perforated Surface," *Proceedings of Transducers'01*, (Munich, Germany), pp. 1506–1509, June 2001.

[3] M. Bao, H. Yang, Y. Sun, and Y. Wang, "Squeeze-film Air Damping of Thick Hole-Plate," *Sensors and Actuators A*, vol. 108, pp. 212–217, 2003.

[4] D. Homentcovschi and R. N. Miles, "Modeling of Viscous Damping of Perforated Planar Microstructures, Applications in Acoustics," *Journal of the Acoustical Society of America*, vol. 116, pp. 2939–2947, November 2004.

[5] R. Sattler and G. Wachutka, "Analytical Compact Models for Squeezed-Film Damping," *Symposium on Design, Test, Integration and Packaging of MEMS/MOEMS, DTIP 2004*, (Montreux), pp. 377–382, May 2004.

[6] T. Veijola, "Analytic Damping Model for an MEM Perforation Cell," *Microfluidics and Nanofluidics*, vol. 2, no. 2, 2006. In print.

[7] P. Råback, A. Pursula, V. Junttila, and T. Veijola, "Hierarchical Finite Element Simulation of Perforated Plates with Arbitrary Hole Geometry," *Proceedings of the 6th International Conference on Modeling and Simulation of Microsystems*, vol. 1, (San Francisco), pp. 194–197, February 2003.

[8] Y.-J. Yang and C.-J. Yu, "Macromodel Extraction of Gas Damping Effects for Perforated Surfaces with Arbitrary-Shaped Geometries," *Proceedings of the 5th International Conference on Modeling and Simulation of Microsystems*, (San Juan, PR), pp. 178–181, April 2002.

[9] T. Veijola and P. Råback, "A Method for Solving Arbitrary MEMS Perforation Problems with Rare Gas Effects," *Proceedings of the 8th International Conference on Modeling and Simulation of Microsystems*, vol. 3, (Anaheim), pp. 561–564, May 2005.

[10] F. Sharipov and V. Seleznev, "Data on Internal Rarefied Gas Flows," *J. Phys. Chem. Ref. Data*, vol. 27, no. 3, pp. 657–706, 1998.

[11] T. Veijola, A. Pursula, and P. Råback, "Extending the Validity of Existing Squeezed-Film Damper Models with Elongations of Surface Dimensions," *Journal of Micromechanics and Microengineering*, vol. 15, pp. 1624–1636, 2005.

[12] "Elmer – Finite Element Solver for Multiphysical Problems." http://www.csc.fi/elmer.

 ISBN: 2-916187-03-0

Appendix

The flow resistance R_P of the perforation cell in Eq. (1) consists of lumped flow resistances and their effective elongations. The equations have been derived partly analytically, partly by fitting the model to FEM simulations by varying the coefficients in heuristic equations [6]:

$$R_\mathrm{S} = \frac{12\pi\eta r_\mathrm{x}^4}{Q_\mathrm{ch} h^3}\left(\frac{1}{2}\ln\frac{r_\mathrm{x}}{r_0} - \frac{3}{8} + \frac{r_0^2}{2r_\mathrm{x}^2} - \frac{r_0^4}{8r_\mathrm{x}^4},\right)$$

$$R_\mathrm{IS} = \frac{6\pi\eta(r_\mathrm{x}^2 - r_0^2)^2}{r_0 h^2}\Delta_\mathrm{S},$$

$$R_\mathrm{IB} = 8\pi\eta r_0 \Delta_\mathrm{B},$$

$$R_\mathrm{IC} = 8\pi\eta r_0 \Delta_\mathrm{C},$$

$$R_\mathrm{C} = \frac{8\pi\eta h_\mathrm{c}}{Q_\mathrm{tb}},$$

and

$$R_\mathrm{E} = 8\pi\eta\Delta_\mathrm{E} r_0.$$

The effective elongations in the previous equations are:

$$\Delta_\mathrm{S} = \frac{0.56 - 0.32\frac{r_0}{r_\mathrm{x}} + 0.86\frac{r_0^2}{r_\mathrm{x}^2}}{1 + 2.5K_\mathrm{ch}},$$

$$\Delta_\mathrm{B} = 1.33\left(1 - 0.812\frac{r_0^2}{r_\mathrm{x}^2}\right)\frac{1 + 0.732K_\mathrm{tb}}{1 + K_\mathrm{ch}} f_\mathrm{B}\left(\frac{r_0}{h}, \frac{h_\mathrm{c}}{h}\right),$$

where

$$f_\mathrm{B}(x, y) = 1 + \frac{x^4 y^3}{7.11(43y^3 + 1)},$$

$$\Delta_\mathrm{C} = (1 + 0.6K_\mathrm{tb})\left(0.66 - 0.41\frac{r_0}{r_\mathrm{x}} - 0.25\frac{r_0^2}{r_\mathrm{x}^2}\right),$$

$$\begin{aligned}\Delta_\mathrm{E} &= \frac{0.944 \cdot 3\pi(1 + 0.216K_\mathrm{tb})}{16} \\ &\times \left(1 + 0.2\frac{r_0^2}{r_x^2} - 0.754\frac{r_0^4}{r_x^4}\right) f_\mathrm{E}\left(\frac{r_0}{h}\right),\end{aligned}$$

where

$$f_\mathrm{E}(x) = 1 + \frac{x^{3.5}}{178(1 + 17.5K_\mathrm{ch})}.$$

 ISBN: 2-916187-03-0